Soft Matter

Accepted Manuscript

ROYAL SOCIETY OF CHEMISTRY

www.rsc.org/softmatter

Soft Matter

COMMUNICATION

Wetting Behavior on Hexagonally Closed-packed Polystyrene Bead Arrays with Different Topographies

Yi-Seul Park,[‡] Seo Young Yoon,[‡] and Jin Seok Lee[*]

Received 00th January 20xx,
Accepted 00th January 20xx

DOI: 10.1039/x0xx00000x

www.rsc.org/

Here, we investigated the wetting behavior of hexagonally close-packed polystyrene bead arrays with different bead diameter and surface flatness. The contact angle was found to be influenced by the surface roughness as well as the contact area of the polystyrene bead array with the water droplet.

The wettability of a solid surface by a liquid is one of the most important surface properties. The contact angle (CA) of water on ideal smooth surfaces is defined by Young's equation and the limit for chemical hydrophobicity is defined as ~120°.[1,2] On the other hand, in the case of non-ideal rough surfaces, two types of surface states are defined, namely the Wenzel state and the Cassie state. In the Wenzel state, the surface is completely wetted by the liquid,[3] whereas in the Cassie state, air is entrapped in the roughness of the substrate and only top areas of the surface are wetted.[4] Therefore, based on the consideration that the wetting behavior is governed by the liquid-solid interface,[1] there have been many efforts to modify the chemical composition and roughness of solid surfaces and investigate the correlation between wetting behavior and surface topography.[5-9] Recently, surface properties have been modified to obtain bioinspired nanostructures mimicking nature such as antireflection in butterfly wings and moth eyes,[10,11] hydrophobicity-based self-cleaning in lotus,[12] and geometry of fibers-based adhesion in gecko.[13] These modified surfaces facilitate the advanced application related with various industry fields. Particularly, the technique for self-cleaning, which are dependent on hydrophobic and hydrophilic properties on surface, is the most important to improve the device performance by moving water drop collects a... removing contaminants from the surface.

To design the surface topography of a solid, many groups have investigated the fabrication of substrates with nano- or microscale topography through various meth ods such as e beam lithography[14,15] and focused ion beam milling techniques.[16,17] In particular, e-beam lithography can precisely control the surface topography on the order of nanometers. However, this technique can only be applied to small areas, and involves high production costs and time.[18]

The organization of building blocks can also produce nano- or micro-structured substrates. Common approaches for the organization of building blocks are based on the self-assembly of coatings on the substrates from a solution phase and include techniques such as sedimentation,[19] evaporation,[20] adsorption,[21] Langmuir–Blodgett,[22] and spin coating.[23] Although these self-assembly methods are useful in organizing colloidal particles into hexagonally ordered arrays using solvents, the organization of building blocks into large and perfect 2D arrays based on self-assembly from solutions has several drawbacks.[24] For instance, defects may easily be formed in the self-assembled arrays, as these arrays are fragile. In addition, only a part of the array may be organized as required or the array formation may proceed in an uncontrolled manner. Moreover, the formation of close-packed arrays over a large area is difficult, and involves considerable time and combined efforts. For accurate CA measurements, the surface of the substrate is required to be homogeneous over an area spanning at least the size of a water droplet.

Owing to the above disadvantages of the self-assembly techniques, manual assembly is advantageous over self-assembly.[25,26] In particular, template-assisted manual assembly is powerful and effective for the organization of building blocks with a large area and with perfect packing.[27] Very fast organization of the building blocks into large and perfect 1D and 2D arrays achieved by the rubbing of dry building blocks on patterned nanowell arrays has been demonstrated.

[*] Department of Chemistry, Sookmyung Women's University
Seoul 140-742 (Korea)
E-mail: jinslee@sookmyung.ac.kr
Homepage: http://fetns.sookmyung.ac.kr
[‡] These authors contributed equally.
† Electronic supplementary information (ESI) available. Experimental details, Figure S1-S5. See DOI: 10.1039/c000000x/

In this study, we measured the CA of water on a hexagonal close-packed (HCP) polystyrene (PS) bead array, which functioned as a micro-structured surface. For precise CA measurements, the HCP PS bead array was formed using a template-assisted manual assembly technique. CA increased with increase in the diameter of the beads as well as increase in the contact area between the water droplet and the PS bead array, which influenced the surface roughness and wetting area. Changes in the surface topography including increased diameter and modified flattened morphology of the PS beads induced large CA, resulting in enhancement in the hydrophobic properties of PS. We surpassed the limit for chemical hydrophobicity by means of this micro-structured surface, and demonstrated the importance of surface roughness and wetting area with increasing hydrophobicity on extensively ordered micro-structured surfaces.

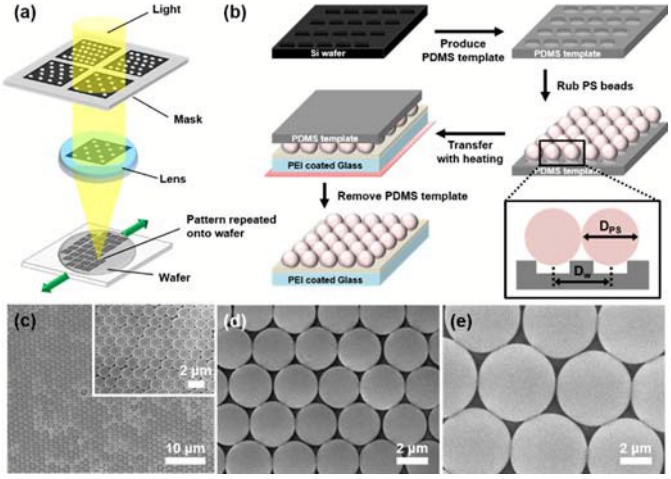

Fig. 1. (a) Schematic diagrams of the production of a patterned Si wafer using the KrF stepping method, and (b) template-assisted manual assembly and thermal transfer procedure of the PS beads. The PDMS template with hexagonal array of wells was formed using a patterned Si wafer. The distance between the wells in the PDMS template and diameter of the PS beads are denoted as D_w and D_{PS}, respectively. The PEI coated glass substrate was kept at 70 °C on hot plate during the transfer process. (c–e) SEM images of the hexagonally close-packed PS bead arrays with different sizes, (c) 1, (d) 3, and (e) 5 μm. These samples are denoted as PS-1, PS-3, and PS-5, respectively. The scale bar for (c) is 10 μm and those for the others (d, e) including the inset in (c) are 2 μm.

To organize the PS beads into a highly ordered HCP monolayer as a micro-structured surface, we fabricated a hexagonally patterned Si wafer as a template using KrF stepper lithography (**Fig. 1a**), and subsequently induced template-assisted manual assembly with the PS beads.[26,27] First, light was passed through the mask with hexagonal arrays pattern of holes, forming an image of the mask pattern. The image was focused and reduced by a lens, and projected onto the surface of a Si wafer that was coated with a photoresist. At this time, the size of pattern image in the mask was reduced fourfold compared to the original pattern area. As a result, the patterned Si wafer with hexagonal arrays of pillars was produced and used as a scaffold for preparation of the poly(dimethylsiloxane) (PDMS) template (**Fig. 1b**). The PS beads, as building blocks for micro-structured surface, were synthesized in various sizes by controlling reagent concentrations such as the concentration of the initiator and capping material (**Fig. S1** and **S2** in ESI).[28-32] These PS beads with different sizes from 1 to 7 μm were organized into a HCP monolayer on the poly(ethyleneimine) (PEI) coated glass substrates by template-assisted manual assembly using the PDMS template with hexagonal array of wells. The PS bead arrays had the bead sizes of 1, 3, 5, and 7 μm and are denoted by PS-1, PS-3, PS-5, and PS-7, respectively. SEM images of the monolayer are shown in **Fig. 1c-e** and **Fig. S4** in ESI.

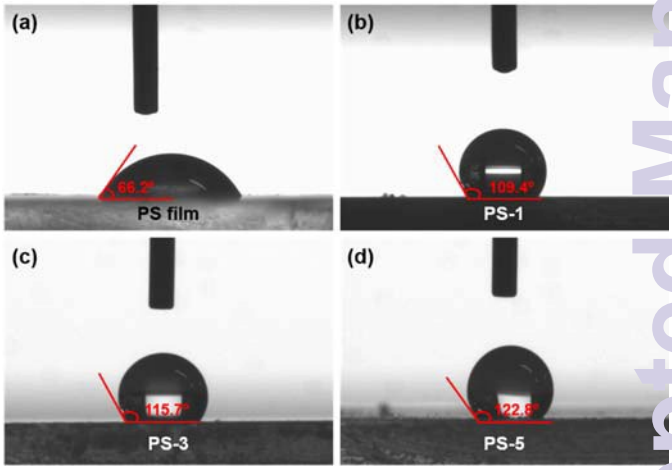

Fig. 2. CA measurements on (a) flat PS film and the hexagonally close-packed (b) PS-1, (c) PS-3, and (d) PS-5 bead arrays.

Previous researchers have demonstrated that manual assembly is a highly effective method for assembling micro-sized building blocks on flat substrates.[26,27] Furthermore, the area having perfectly packed organization drastically increases with template-assisted manual assembly. In general, this manual assembly process can be affected by the properties of the PS beads such as their diameter and the extent of aggregation. Thus, the PS beads should not be aggregated and their diameter, D_{PS}, must correspond to the distance between the centers of the wells in the PDMS template, denoted by D_w. The unequal PS beads, with diameters larger or smaller than the average diameter of the population (D_{PS}), disrupt the close packing of the PS beads and induce defects in the PS bead array (**Fig. S3** in ESI). In the case of the PS beads where D_{PS} is larger than the D_w of the PDMS template ($D_{PS} > D_w$), assembly of the beads into a perfect close-packed structure is difficult because the size of the beads causes them to overflow into the neighboring wells of the PDMS template. On the other hand, the PS beads with diameters smaller than the D_w of the PDMS template ($D_{PS} < D_w$) are embedded into the wells of the template, which deform the wells of the soft and easily bendable PDMS template from a spherical to an oval shape, causing defects in the PS bead assembly. Therefore, controlling the size of the PS

beads in a narrow size distribution is important for organizing the beads into a perfect HCP monolayer assembly.

In order to understand the influence of the diameter of the PS beads on the surface wettability, the CA of water on flat PS films as well as PS bead arrays were measured, as shown in **Fig. 2** and **Fig. S4d** in ESI. The flat PS film showed a water CA of 66.2°. However, in the case of the PS bead arrays, the CAs were larger than that of the flat PS surface. In addition, the CAs of the PS bead arrays gradually increased to 109.4°, 115.7°, 122.8°, and 136.5° for samples PS-1, PS-3, PS-5, and PS-7, respectively, with increase in the diameter of the PS beads. In agreement with calculation using Young's equation,[2] the CA of water on a flat PS surface was obtained. But, this equation is not applicable to non-ideal rough surfaces such as PS bead arrays.[9] It has been shown in a previous study that the experimental CA measurements on a micro-structured surface are closer to the values of the calculated Cassie-Baxter CA (θ_{CB}) than that of the Wenzel CA.[33] The Cassie-Baxter CA, θ_{CB}, is defined as follows.[9]

$$\cos\theta_{CB} = f_{sl} (r_f \cdot \cos\theta_{flat} + 1) - 1 \quad (1)$$

In the above equation, f_{sl} is the fraction of the droplet in contact with the surface and r_f is the roughness factor defined as the ratio of the actual surface area of the rough surface to the surface projected area. And, θ_{flat} is the CA of water on the flat surface of corresponding material.

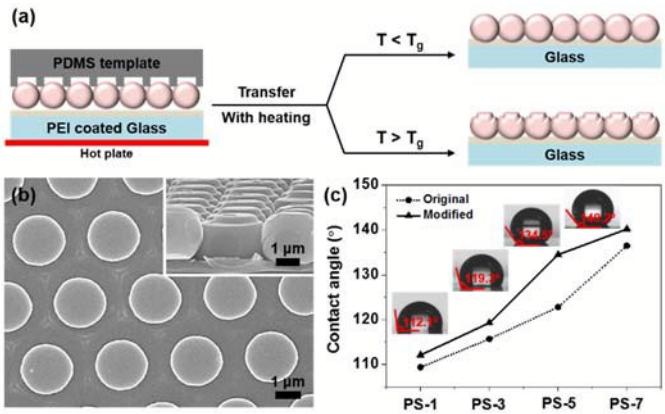

Fig. 3. (a) Schematic diagram of the surface modification process of the PS bead arrays by a thermal imprinting method. The PEI coated glass substrate was kept on the hotplate heated below (70 °C) or above T_g (150 °C) of PS during the transfer process, to control the surface flatness of PS bead arrays. (b) SEM image (top-view) of the modified surface of PS-3. The scale bar is 1 μm. Inset shows a SEM image (tilt-view) of the modified surface of PS-3. (c) Comparison of the contact angle of water on the original and modified PS bead arrays.

The roughness of a solid surface can influence its surface wetting properties, in addition to the chemical composition of the surface and the properties of the liquid.[1] While the PS surface is hydrophobic by itself, the roughness introduced by the PS bead array further increased the hydrophobicity of the PS surface, which explains why the CAs of water on the PS bead arrays were larger than that on the PS flat film. Furthermore, the CAs tended to increase with increase in the diameter of the PS beads. The diameter of the PS beads in the arrays led to increase in roughness (r_f) in equation (1). The surface roughness was measured using atomic force microscopy (AFM), whose root-mean square (RMS) values are 0.168, 0.470, 0.768, and 0.890 μm for PS-1, PS-3, PS-5, and PS-7, respectively (**Fig. S5** in ESI). The surface roughness increases by increasing the diameter of PS beads, consistent with results from equations. Consequently, the CA increased with the diameter of PS beads.

In order to investigate the effect of the fraction of the water droplet in contact with the substrate (f_{sl}) on the CA measurement for a given diameter of PS beads, the top surfaces of the PS bead arrays were modified by a thermal imprinting method. When the PS beads are transferred from the PDMS template to the PEI coated glass substrates, the PEI layer needs to be soft to act as a molecular glue for the PS beads by heating above the glass transition temperature (T_g) of PEI.[27] In order to modify the top surface of the PS bead arrays in contact with the water droplet, temperature above T_g of PS (150 °C) was used during the thermal imprinting process, which made the PS beads soft, in addition to the PEI layer. In addition, a mark of the PDMS template structure, like as the cylindrical well array, was imprinted on the top surfaces of the PS beads due to the physical force involved in the transfer (**Fig. 3a**). As a result, the modified PS bead arrays had different surface topographies, like as the cylindrical pillar array, compared to the original PS bead arrays (**Fig. 3b**). When the CA was measured, the water droplet was in contact with the top of the PS beads in both cases. However, in the case of the modified PS beads, the contact area of water was larger due to the flattened top of the PS beads.

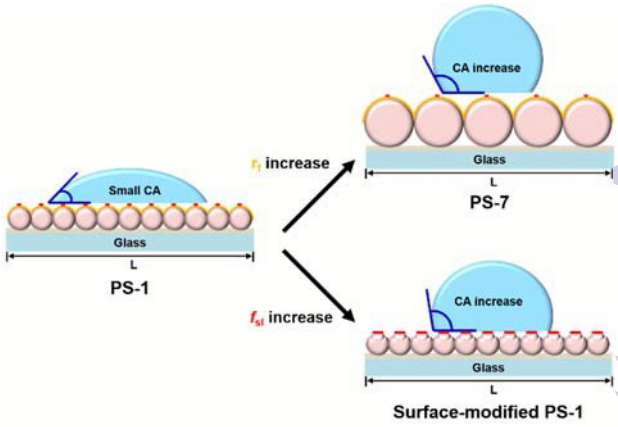

Fig. 4. Schematic diagram of CA changes with change in surface roughness (r_f) and fraction of contact area (f_{sl}) of the PS bead array for identical area (L). The surface roughness and fraction of contact area are represented in orange and red, respectively.

The CAs of the modified PS bead arrays increased from 109.4° to 112.1°, 115.7° to 119.3°, 122.8° to 134.5°, and 136.5° to 140.2° for the samples with 1 μm, 3 μm, 5 μm, and 7 μm PS bead diameters, respectively (**Fig. 3c**, solid and dashed lines and **Fig. S4** in ESI). This implies that there was an increase in f_{sl} at the modified PS beads surface compared to the original PS beads surface, according to equation (1), leading to increase in CA of water (**Fig. 3c**). Similar to the original PS bead arrays, the CAs

increased on the modified surface of PS beads with an increase in the diameter of the PS beads. As mentioned previously, the CA of water on a smooth surface cannot exceed ~120°, which is defined as the limit for chemical hydrophobicity. However, the CA of water on the modified surface of PS-7 was measured to be 140.2°, as a result of the surface roughness and flattened top induced by the modification of PS bead array.

Fig. 4 schematically illustrates the key findings based on the CA measurements of both original and modified PS bead arrays. In this study, we showed that the wetting behavior of PS can be changed by controlling its surface topography. The diameter of the PS beads and the flatness of the top of the PS beads significantly influenced the CA of water on the PS bead arrays, due to increase in the roughness (r_f) of the surface and the contact area (f_{sl}) of water on the surface. When the diameter of the PS beads increased, the roughness of the substrate also increased and consequently, the CA was higher on the PS bead arrays having a large diameter. Furthermore, surface modification of the PS beads can also influence the contact area. When the surface of the PS bead array was modified by increasing the temperature at which the PS beads were transferred to the glass substrate above T_g, the contact area of the PS surface with water increased, for a given diameter of the PS beads. The top surface of the PS beads was flattened by a combination of thermal and physical forces during the transfer process, which provided a larger contact area between the PS beads and the water drop, resulting in a higher CA on the modified PS bead array. These results suggest that the contact area between the micro-structured surface and the water drop is an important factor in the CA measurements.

Conclusions

In summary, we investigated the effect of surface roughness and contact area between the PS bead array and water, on the CA measurements. For the CA measurements, we organized the PS beads with different sizes in the range of 1-7 μm into an HCP monolayer using a template-assisted manual assembly technique. It was found that increasing the diameter of the PS beads resulted in an increase in the CA, which is attributed to the increase in surface roughness (r_f) on the PS bead array. Additionally, the contact area (f_{sl}) between the water droplet and the substrate was also increased by surface modification of the PS bead array and it was found that the CA increased with increase in contact area. We believe that our topographical approach provides important insights into the role of surface topography in the wetting behavior of solid materials and a conceptual framework for the design and engineering of interface between liquid and solid materials.

This work was supported by Nano-Material Technology Development Program (2012M3A7B4034986) funded by the National Research Foundation and the Pioneer Research Center Program through the National Research Foundation of Korea funded by the Ministry of Science, ICT & Future Planning (2012-0009562). Additionally, it was supported by the Basic Science Research Program through the National Research Foundation of Korea (NRF) funded by the Ministry of Science, ICT & Future Planning (2015R1A2A2A01005556).

Notes and references

1 H. Teisala, M. Tuominen, J. Kuusipalo, *Adv. Mater. Interfaces* 2014, **1**, 1300026.
2 T. Young, *Philos. Trans. R. Soc. London* 1805, **95**, 65–87.
3 R. N. Wenzel, *Ind. Eng. Chem.* 1936, **28**, 988–994.
4 A. B. D. Cassie, S. Baxter, *Trans. Faraday Soc.* 1944, **40**, 546–551.
5 G. McHale, N. J. Shirtcliffe, M. I. Newton, *Langmuir* 2004, **20**, 10146–10149.
6 T. Onda, S. Shibuichi, N. Satoh, K. Tsujii, *Langmuir* 1996, **12**, 2125–2127.
7 C. Neinhuis, W. Barthlott, *Ann. Bot.* 1997, **79**, 667–677.
8 R. Blossey, *Nat. Mater*. 2003, **2**, 301–306.
9 S. Moradi, P. Englezos, S. G. Hatzikiriakos, *Colloid Polym. Sci.* 2013, **291**, 317–328.
10 Q. Zhao, T. Fan, J. Ding, D. Zhang, Q. Guo, M. Kamada, *Carbon* 2011, **49**, 877–883.
11 S. Ji, K. Song, T. B. Nguyen, N. Kim, H. Lim, *ACS Appl. Mat. Interfaces* 2013, **5**, 10731–10737.
12 Y. Yoon, D. Kim, J. –B. Lee, *Micro and Nano Systems Lett.* 2014, **2**, 3.
13 M. Zhou, N. Pesika, H. Zeng, Y. Tian, J. Israelachvili, *Friction* 2013, **1**, 114–129.
14 S. Donthu, S. Pan, B. Myers, G. Shekhawat, G. N. Wu, V. Dravid, *Nano Lett.* 2005, **5**, 1710-1715.
15 R. Glass, M. Arnold, J. Blümmel, A. Küller, M. Möller, J. P. Spatz, *Adv. Funct. Mater.* 2003, **13**, 569–575.
16 K. Arshak, M. Mihov, A. Arshak, D. McDonagh, D. Sutton, *Microelectron. Eng.* 2004, **73**, 144–151.
17 M. J. Cryan, M. Hill, D. C. Sanz, P. S. Ivanov, P. J. Heard, L. Tian, S. Yu, J. M. Rorison, *IEEE J. Sel. Top. Quant.* 2005, **11**, 1266-1276.
18 H. Cao, Z. Yu, J. Wang, J. O. Tegenfeldt, R. H. Austin, E. Chen W. Wu, S. Y. Chou, *Appl. Phys. Lett.* 2002, **81**, 174–176.
19 R. Micheletto, H. Fukuda, M. Ohtsu, *Langmuir* 1995, **11**, 3333–3336.
20 P. Jiang, J. F. Bertone, K. S. Hwang, V. L. Colvin, *Chem. Mater.* 1999, **11**, 2132–2140.
21 C. E. Snyder, A. M. Yake, J. D. Feick, D. Velegol, D. *Langmuir* 2005, **21**, 4813–4815.
22 M. Bardosova, M. E. Pemble, I. M. Povey, R. H. Tredgold, *Adv Mater.* 2010, **22**, 3104–3124.
23 P. Jiang, M. J. McFarland, *J. Am. Chem. Soc.* 2004, **126**, 13778–13786.
24 Y. -H. Ye, S. Badilescu, V. -V. Truong, P. Rochon, A. Natansohn *Appl. Phys. Lett*. 2001, **79**, 872–874.
25 K. B. Yoon, *Acc. Chem. Res.* 2007, **40**, 29–40.
26 J. S. Lee, J. H. Kim, Y. J. Lee, N. C. Jeong, K. B. Yoon, *Angew Chem. Int. Ed.* 2007, **46**, 3087–3090.
27 N. N. Khanh, K. B. Yoon, *J. Am. Chem. Soc.* 2009, **131**, 1422[illegible] 14230.
28 C. –S. Chern, C. –H. Lin, *Polymer* 2000, **41**, 4473–4481.
29 T. Yamamoto, M. Iuoue, Y. Kanda, K. Higashitani, *Chem. Lett.* 2004, **33**, 1440–1441.
30 A. J. Paine, *Colloid Interface Sci.* 1990, **138**, 157–169.
31 S. H. Im, G. E. Khalil, J. Callis, B. H. Ahn, M. Gouterman, Y. X[illegible] *Talanta* 2005, **67**, 492–497.
32 T. Yamamoto, M. Nakayama, Y. Kanda, K. Higashitani, J *Colloid Interface Sci.* 2006, **297**, 112–121.
33 B. Bhushan, Y. C. Jung, K. Koch, *Phil. Trans. R. Soc. A* 2009, **367**, 1631–1672.

Table Of Contents (TOC)

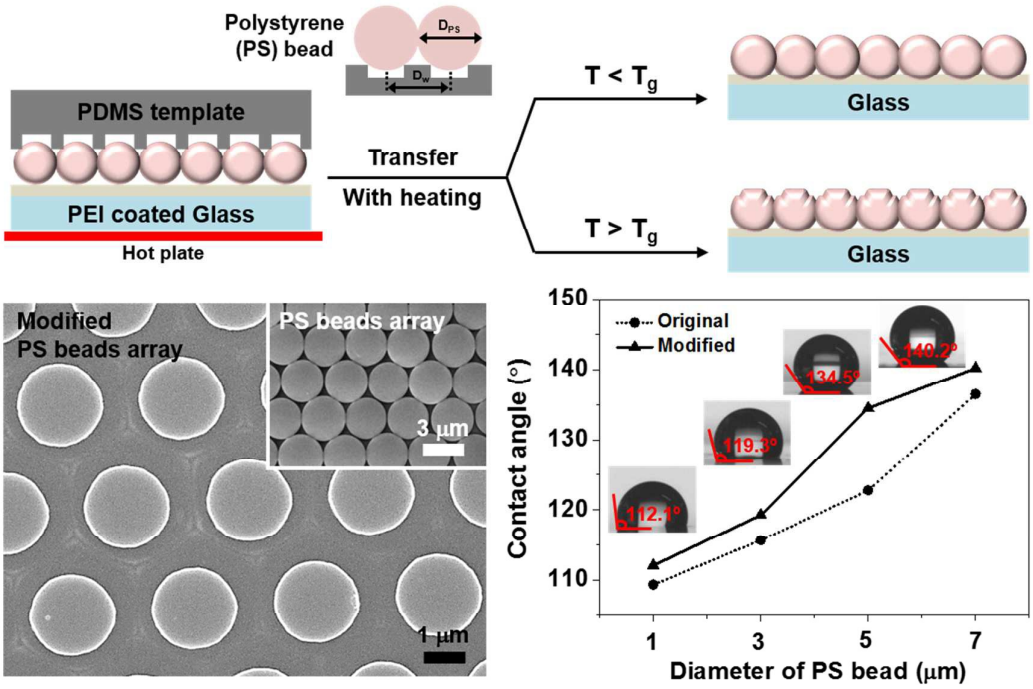

The wetting behavior of polystyrene beads array is influenced by the surface roughness and the contact area with water droplet.